Effect of the Particle Size on Asphaltene Adsorption and Catalytic Oxidation onto Alumina Particles

ARTICLE *in* ENERGY & FUELS · AUGUST 2011

Impact Factor: 2.79 · DOI: 10.1021/ef2008387

3 AUTHORS, INCLUDING:

Nashaat N Nassar
The University of Calgary
64 PUBLICATIONS **885** CITATIONS

SEE PROFILE

Azfar Hassan
The University of Calgary
36 PUBLICATIONS **386** CITATIONS

SEE PROFILE

energy&fuels

ARTICLE

pubs.acs.org/EF

Effect of the Particle Size on Asphaltene Adsorption and Catalytic Oxidation onto Alumina Particles

Nashaat N. Nassar,* Azfar Hassan, and Pedro Pereira-Almao

Department of Chemical and Petroleum Engineering, University of Calgary, Calgary, Alberta T2N 1N4, Canada

ABSTRACT: In this study, the adsorption and catalytic oxidation of asphaltenes, problematic heavy hydrocarbons present in heavy oil, onto two aluminas with different particle sizes and comparable surface acidity were investigated. Equilibrium batch adsorption experiments were conducted at 25 °C with solutions of asphaltenes in toluene at concentrations ranging from 100 to 3000 mg/L. Adsorption data were fit to the Langmuir and Freundlich isotherm models. Nano-alumina fit better to the Langmuir model, while micro-alumina fit well to the Freundlich model. On a surface area basis, nano-alumina has higher adsorption capacity for asphaltenes than micro-alumina. Interestingly, micro-alumina has higher catalytic activity toward asphaltene oxidation than nano-alumina, at the same asphaltene loading, thus exhibiting the significance of textural properties during catalytic oxidation of asphaltenes that dominated over the effect of the particle size.

1. INTRODUCTION

With the rapid increase in global energy demands and the depletion of the conventional oil, the search for alternative environmentally friendly and sustainable fuels or energy sources has become highly pronounced in the current context.[1] Oil sands resources have shown potential to be one of the reliable supplies.[2] However, a number of factors play a major role in determining the level of oil sands contribution, including cost of extraction and the technology of the extraction process, as well as the environmental impact of the current processes of oil sands extraction and exploration. To meet global energy demands while appropriately addressing environmental concerns, there is a strong need to develop environmentally friendly, cost-effective, efficient, innovative, and smart technologies for oil sands exploration and extraction.[3−6] Nanotechnology has potential solutions to many of the challenges facing the oil sands industry. Recently, we have successfully employed different metal oxide nanoparticles for heavy oil upgrading, H_2S capture, adsorptive removal of heavy hydrocarbons, and catalytic oxidation and steam gasification of asphaltenes, typical problematic heavy hydrocarbons.[3−5,7,8] The adsorption behavior and catalytic activities of different metal oxide nanoparticles toward asphaltene adsorption, oxidation, and gasification/cracking have been addressed.[3−5] We also investigated the effect of surface acidity and basicity of adsorbent/catalyst on the adsorption and oxidation of asphaltenes.[9] Our results showed that asphaltene adsorption, oxidation, and gasification/cracking are metal-oxide-specific and more strongly influenced by surface acidity or basicity. The acidic surface has the highest adsorption of asphaltenes, while basic surface has the highest catalytic activity toward asphaltene oxidation. The objective of this study is to compare the adsorptive and catalytic properties of asphaltenes onto macro- and nanometer scale alumina particles to study the effect of the particle size on the adsorption and oxidation processes. For this purpose, two types of aluminas having similar surface acidity but differing in particle size were employed for asphaltene adsorption and, subsequent, catalytic oxidation of the adsorbed asphaltenes. To the best of our knowledge, a work-relating effect of the particle size on asphaltene adsorption and catalytic oxidation is conducted for the first time. This study will provide valuable insight on the size effect of adsorbent/catalyst toward asphaltene adsorption and oxidation, which is crucial for the heavy oil industry.

2. EXPERIMENTAL SECTION

2.1. Alumina Particles. Alumina nanoparticles were obtained from Sigma−Aldrich. Its reported particle size is <50 nm. Alumina microparticles were obtained from Sorbent Technologies, Inc., Atlanta, GA), and its reported particle size is between 50 and 200 μm. The particles were used without further purification.

2.2. Surface Area and Particle Size Measurements. The surface areas of both alumina adsorbents were estimated following the Brunauer−Emmett−Teller (BET) method. This was achieved by performing nitrogen adsorption−desorption at 77 K, using a Micromeretics Tristar 2000 surface area analyzer. The samples were degassed at 150 °C under N_2 flow overnight before analysis. Surface areas were calculated using the BET equation. The size of the particles was determined using an X-ray Ultima III multi-purpose diffraction system (Rigaku Corp., The Woodlands, TX), with Cu Kα radiation operating at 40 kV and 44 mA with a $\theta/2\theta$ goniometer.

2.3. Temperature-Programmed Desorption of Ammonia (NH_3-TPD). The surface acidity/basicity of the aluminas was measured using the NH_3-TPD setup. NH_3-TPD experiments were carried out using Quantachrome ChemBet 3000 to measure total surface acidity of aluminas studied. Because we are targeting adsorption of asphaltene molecules over the alumina support, surface acidity becomes an important parameter to be measured. Ammonia is a strong base ($pK_b \approx 5$) that reacts even with extremely weak acid sites, which therefore makes NH_3-TPD a useful technique for evaluating the relative amount of acid sites present on a surface. NH_3 peak calibration was first carried out followed by TPD of NH_3 for various solids. NH_3-TPD measurements were performed using gases of ultra-high purity (UHP) grade. About 100 mg of sample was introduced in the cylindrical glass TPD

Received: June 7, 2011
Revised: July 19, 2011
Published: August 01, 2011

Table 1. Characteristics of Selected Alumina Particles

type	X-ray measured particle size	specific surface area (BET) (m^2/g)	pore volume (cm^3/g)	average pore size (Å)
nano	48 ± 3 nm	39		
micro	<200 μm	156	0.2909	54

microreactor (2 mm internal diameter), which is then degassed at 150 °C overnight under He flow maintained at atmospheric pressure. The sample was cooled to 100 °C, and NH_3 (10% in He) was introduced through the sample fixed bed for 1 h. Physisorbed NH_3 was then removed by He flow over the solid for about 1 h at 100 °C. The sample was then heated to 900 °C at a linear rate of 10 K/min for desorption of the chemisorbed NH_3. The amount of NH_3 that is desorbed as a function of the temperature is calculated on the basis of the peak area using a calibration curve made for this purpose. The amount of NH_3 desorbed is therefore an indication of the total acidity of the solid.

2.4. Asphaltenes. The asphaltenes obtained from the Athabasca bitumen sample in Alberta were used as an adsorbate in this study. Asphaltenes were extracted from the bitumen sample with the addition of *n*-heptane [99% high-performance liquid chromatography (HPLC) grade, Sigma Aldrich, Ontario, Canada], following the technique described in previous studies.[5,10]

2.5. Heavy Oil Model Solutions. The heavy oil model solutions for the batch adsorption experiments were prepared by dissolving a specified amount of the asphaltenes in toluene (analytical grade, EMD Chemicals, Inc., Merck, Gibbstown, NJ). The initial concentration of asphaltenes in solution used in the adsorption experiments ranged from 100 to 3000 mg/L.

2.6. Equilibrium Adsorption Isotherms. Batch adsorption experiments were carried out in 20 mL vials by mixing together 100 mg of alumina particles with 10 mL of the prepared heavy oil solution at 25 °C. The contents in the vials were agitated at 200 rpm by placing them in a temperature incubator and allowing them to equilibrate for 24 h, which was an adequate time to achieve equilibrium.[5,10] The mixture was then centrifuged at 5000 rpm for 30 min to remove the alumina particles. Then, the alumina particles containing adsorbed asphaltenes were placed in a vacuum oven at 65 °C for 24 h to evaporate any remaining toluene. After that, the particles were analyzed for their asphaltene content using a thermogravimetric analysis/differential scanning calorimetry (TGA/DSC) analyzer (SDT Q600, TA Instruments, Inc., New Castle, DE).

2.7. Adsorption Modeling. Adsorption isotherms of different of asphaltenes onto different alumina particles were modeled using the Freundlich and Langmuir models presented in eqs 1 and 2, respectively

$$Q_e = Q_{max}\frac{K_L C_e}{1 + K_L C_e} \quad (1)$$

$$Q_e = K_F C_e^{1/n} \quad (2)$$

where Q_e is the equilibrium adsorbed amount of asphaltenes onto the alumina particles (mg/g), C_e is the equilibrium concentration of asphaltenes in the supernatant (mg/L), K_L is the Langmuir equilibrium adsorption constant related to the affinity of adsorption (L/mg), Q_{max} is the maximum adsorbed amount of asphaltenes per mass of alumina particles for complete monolayer coverage (mg/g), K_F is the Freundlich constant related to the adsorption capacity [(mg/g)(L/mg)$^{1/n}$], and $1/n$ is the adsorption intensity factor. The Freundlich and Langmuir constants were estimated from the slopes and intercepts of the linear forms of eqs 1 and 2. The nonlinear χ^2 analyses were conducted for comparing the best-fit model as per eq 3[11]

$$\chi^2 = \sum\frac{(Q_{exp} - Q_{model})^2}{Q_{model}} \quad (3)$$

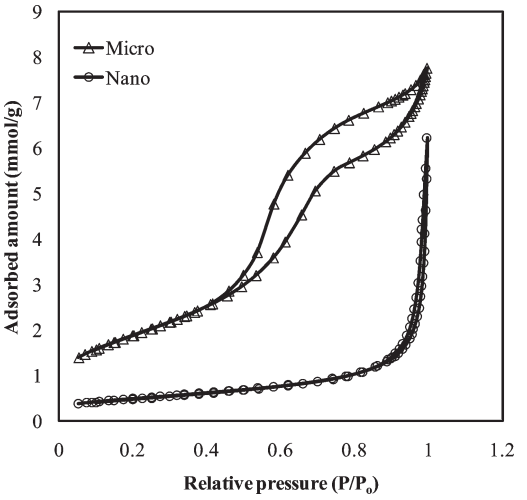

Figure 1. Adsorption−desorption isotherms of N_2 taken at 77 K on nano- and micro-aluminas.

Table 2. Surface Acidity of Aluminas Measured by the NH_3-TPD Method

alumina	NH_3 uptake (μmol/g)	NH_3 uptake (μmol/m^2)
nano	195	5.0
micro	733	4.8

where Q_{exp} and Q_{model} are the equilibrium adsorbed amount of asphaltenes obtained experimentally and modeling, respectively.

2.8. Oxidation and Thermal Analysis of Asphaltenes. Simultaneous thermal analysis of asphaltenes with and without alumina particles was carried out using TGA. About 5−10 mg of sample was heated under air atmosphere. The flow rate of air was kept at 100 cm^3/min. The sample was heated to 1000 °C at a heating rate of 10 °C/min.

3. RESULTS AND DISCUSSION

3.1. Textural Properties of the Selected Alumina Particles. The textural properties of the particles, including particle size and BET, are presented in Table 1. Figure 1 shows the N_2 adsorption−desorption isotherms for micro- and nano-aluminas. According to the classifications of the International Union of Pure and Applied Chemistry (IUPAC), the shape of the isotherm of micro-alumina is a typical type-IV pattern that indicates mesoporous characteristics.[12] The hysteresis loop of this isotherm is associated with the filling and emptying of the mesopores by capillary condensation. As shown in Figure 1, the hysteresis loop was found in micro-alumina, while nano-alumina did not show any hysteresis because of its nonporous structure.

3.2. Surface Acidity of Alumina Particles. Surface acidity of aluminas measured by the NH_3-TPD method are given in Table 2. It appears that micro- and nano-aluminas have comparable surface acidity. The total NH_3 uptake in terms of μmol/g is high for micro-alumina because of the high surface area and does not relate directly to the surface acidity of the material.

3.3. Adsorption Isotherms. It should be noted that the adsorbed amount of asphaltenes onto different sizes of alumina were presented on a surface area basis (i.e., mg/m^2). This is expected to provide better insight on the effect of particle size

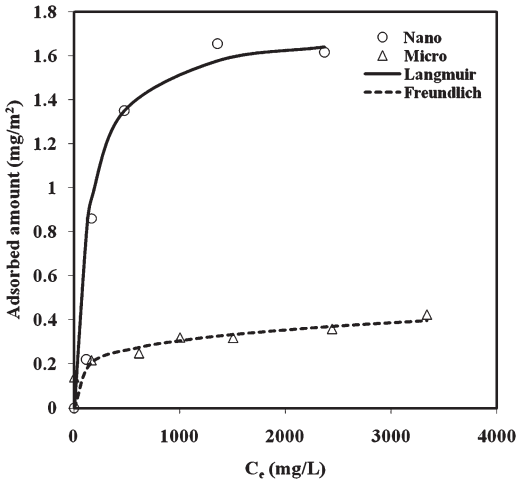

Figure 2. Adsorption isotherms of asphaltenes onto nano- and micro-alumina adsorbents. Adsorbent dose, 10 g/L; shaking rate, 200 rpm; contact time, 24 h; and temperature, 25 °C. Points are experimental data; the solid line is from the Langmuir model (eq 1); and the dashed line is from the Freundlich model (eq 2).

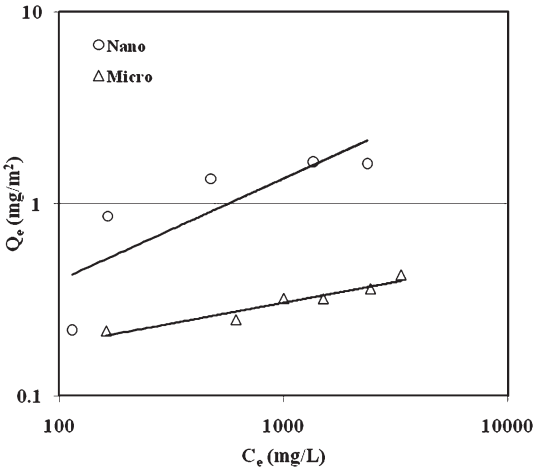

Figure 3. Freundlich isotherms of asphaltenes onto nano- and micro-aluminas. Adsorbent dose, 10 g/L; shaking rate, 200 rpm; contact time, 24 h; and temperature, 25 °C.

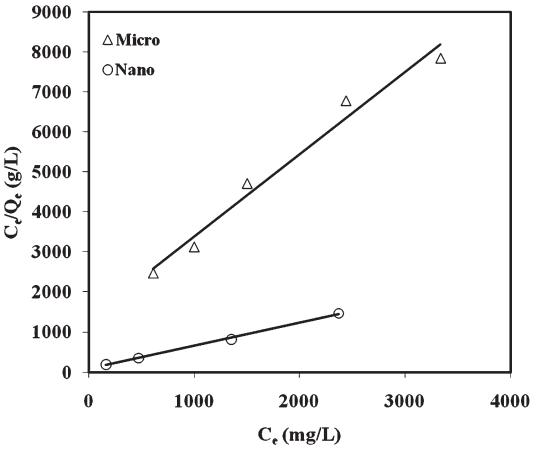

Figure 4. Langmuir isotherms of asphaltenes onto nano- and micro-aluminas. Adsorbent dose, 10 g/L; shaking rate, 200 rpm; contact time, 24 h; and temperature, 25 °C.

and dispersion degree on the mechanistic interpretation of asphaltene adsorption onto alumina surfaces. Figure 2 shows the isotherms of asphaltene adsorption onto nano- and micro-aluminas. As seen, both aluminas succeeded in adsorbing asphaltenes with different degrees. Despite the fact that adsorption is expressed by a surface area basis, alumina nanoparticles showed higher adsorption affinity (initial slope of the isotherm curve) and adsorption capacity (position of plateau) in comparison to micro-alumina. This indicates that the increase in adsorption capacity and affinity of alumina with the decrease in the particle size goes beyond the increase in surface area and involves other factors, such as dispersion ability and intrinsic reactivity. To further investigate the adsorption behavior, adsorption isotherms were modeled using the Langmuir and Freundlich models. The linear forms of the Langmuir and Freundlich models are presented in eqs 4 and 5, respectively.

$$\frac{C_e}{Q_e} = \frac{1}{Q_{max}K_L} + \frac{C_e}{Q_{max}} \tag{4}$$

$$\log(Q_e) = \log(K_F) + \frac{1}{n}\log(C_e) \tag{5}$$

Figures 3 and 4 show the experimental data and the Langmuir and Freundlich isotherms of asphaltenes over nano- and micro-alumina surfaces at 25 °C. Table 3 lists the calculated values from the Langmuir and Freundlich isotherms. The adsorption data in Figures 3 and 4 fit well for both the Freundlich and Langmuir models. However, from the χ^2 test analysis (Table 2), the Freundlich model seems to be the best-fit model for micro-alumina, while the Langmuir model is the best-fit model for nano-alumina. It should be noted that the Langmuir model assumes monolayer adsorption on the adsorbent surface with a finite number of identical sites. On the other hand, the Freundlich model is an empirical equation based on adsorption on a heterogeneous surface.

3.4. Catalytic Oxidation of Adsorbed Asphaltenes. Thermal analyses were conducted to obtain more insight on the effect of the particle size on the catalytic oxidation of adsorbed asphaltenes. Catalytic oxidation was performed using the thermogravimetric setup, as described in the Experimental Section. As simultaneous thermal analysis is performed, both mass and heat changes with time are monitored. In this study, the sample mass was kept to a minimum to avoid mass-transfer limitations. The percent conversion ratio or the extent of the reaction (α) was determined from the weight loss data as per the following equation:

$$\alpha = \frac{w_o - w_t}{w_o - w_\infty} \tag{6}$$

where w_o is the initial sample mass, w_∞ is the final sample mass, and w_t is the sample mass at any time. Figure 5 shows the profiles for the percent conversion with the increase in the temperature for virgin asphaltenes as well as for asphaltenes adsorbed over micro- and nano-aluminas. As seen, the profile of virgin asphaltene oxidation can be divided into two main regions. First, a low-temperature range up to 400 °C. Second, a high-temperature

Table 3. Langmuir and Freundlich Constants for Asphaltene Adsorption onto Nano- and Micro-aluminas at 25 °C

	Freundlich constants				Langmuir constants			
adsorbent	K_F [(mg/m^2)(L/mg)$^{1/n}$]	$1/n$	R^2	χ^2	K_L (L/mg)	Q_{max} (mg/m^2)	R^2	χ^2
nano-alumina	0.273	0.241	0.88	0.516	0.0075	1.73	0.998	0.430
micro-alumina	0.069	0.216	0.93	0.007	0.0025	0.448	0.970	0.071

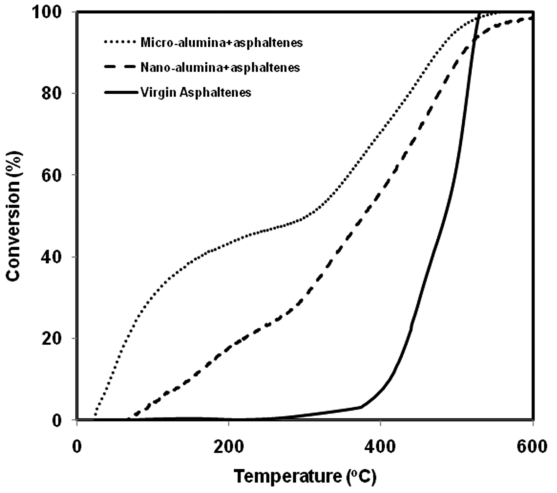

Figure 5. Percent conversion of asphaltenes in the presence and absence of different alumina particles.

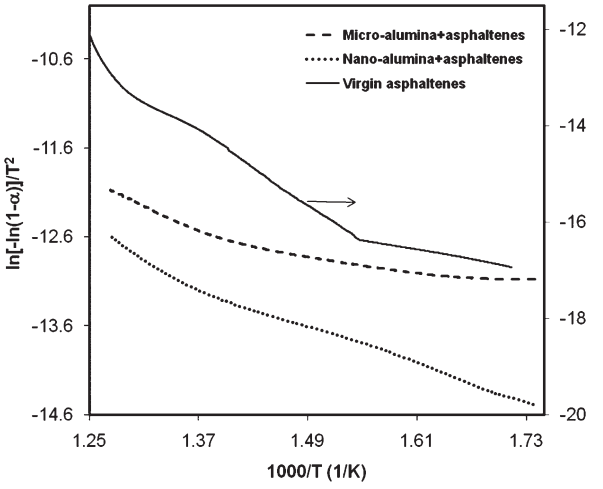

Figure 6. Catalytic oxidation of asphaltenes in the presence and absence of different alumina particles.

range beyond 400 °C. Because asphaltenes are heavy fractions of heavy oil, little mass change was observed during oxidation in the low-temperature range and, therefore, no appreciable conversion can be seen. It appears that thermal decomposition of virgin asphaltenes started beyond 370 °C and reached a maximum rate at around 500 °C, showing the occurrence of combustion reactions during oxidation. As seen in Figure 5, the presence of alumina particles greatly enhanced the asphaltene oxidation, depicting the catalytic effect of the aluminas. Interestingly, although both aluminas have the same loading of asphaltenes per surface area (i.e., 0.22 mg/m^2), micro-alumina has higher catalytic activity in terms of asphaltene percent conversion than nano-alumina. This suggests that the surface area is not the only controlling factor for catalytic activity. It is interesting to note that the two aluminas do not differ in their surface acidity. However, the two aluminas, nano and micro, had different types of adsorption isotherms. Therefore, the number and types of adsorption sites will be different. This would impact the adsorption affinity as well as catalytic activity of the aluminas. The lower catalytic activity of nano-alumina observed in the present work could result from the less number of active sites available for the reaction. This indicates that the surface structure of alumina is more important than the particle size in affecting the catalytic oxidation of asphaltenes.

3.5. Estimation of Activation Energies. The calculation of activation energies was employed to better explain the oxidation reaction and provide more insight into the catalytic effect of different sizes of alumina particles. The activation energies were calculated using the Coats−Redfern method,[13] which is an integral method of processing the TGA data and deals with only one curve of weight loss. A detailed description of this method can be found elsewhere.[13] Briefly, according to the Arrhenius equation, the conversion rate can be expressed by

$$\frac{d\alpha}{dt} = Ae^{-E_a/RT} f(\alpha) \tag{7}$$

where A is the pre-exponential factor (s^{-1}), E_a is the activation energy (kJ/mol), R is the ideal gas constant (8.314 J mol^{-1} K^{-1}), T is the reaction temperature in Kelvin, and $f(\alpha)$ is the reaction mechanism function. The Coats−Redfern method stated that for a reaction mechanism of $f(\alpha) = (1-\alpha)^n$, where n is the order of the reaction, the following expression is obtained after the integration of eq 7:

$$\frac{AR}{\beta E_a}\left(1-\frac{2RT}{E_a}\right)\exp\left(\frac{-E_a}{RT}\right) = \begin{cases} \left(\dfrac{-\ln(1-\alpha)}{T^2},\ n=1\right) \\ \left(\dfrac{1-(1-\alpha)^n}{(1-\alpha)T^2},\ n\neq 1\right) \end{cases} \tag{8}$$

Assuming the value of $2RT/E_a \ll 1$ and taking the natural logarithm on both sides, eq 8 can also be written in linear form as follows:

$$\ln\left(\frac{AR}{\beta E_a}\right) - \frac{E_a}{R}\left(\frac{1}{T}\right) = \begin{cases} \ln\left(\dfrac{-\ln(1-\alpha)}{T^2},\ n=1\right) \\ \ln\left(\dfrac{1-(1-\alpha)^n}{(1-\alpha)T^2},\ n\neq 1\right) \end{cases} \tag{9}$$

If n is known, then a plot of the right-hand side of eq 9 against $1/T$ would give a straight line with a slope = $-E_a/R$. It should be noted that some deviation from the single straight line can occur

Table 4. Activation Energies for Asphaltene Oxidation in the Presence and Absence of Nano- and Micro-aluminas at Different Temperatures

virgin asphaltenes		227−372 °C	372−467 °C	467−514 °C
	E_a (kJ/mol)	42	108	91
	R^2	0.982	0.999	0.98
asphaltenes adsorbed onto alumina			300−443 °C	>450 °C
nano-alumina	E_a (kJ/mol)		16.72	39.83
	R^2		0.9968	0.9984
			330−425 °C	>440 °C
micro-alumina	E_a (kJ/mol)		12.56	38.22
	R^2		0.9874	0.9952

because of the presence of competitive reactions or a change in the reaction mechanism with an increase in the temperature. This will result in multi-straight lines with different slopes and accordingly multi-reactions with different activation energies. Figure 6 shows the plot of $\ln((-\ln(1-\alpha))/(T^2))$ against $1/T$. The values of activation energies for asphaltene oxidation in the presence and absence of alumina particles were determined from the slopes of the best-fit lines. The values determined are listed in Table 4. For virgin asphaltenes, the activation energy was calculated for three distinct temperature regions between 225 and 515 °C. As shown in Table 4, the activation energy and oxidation temperature of asphaltenes decreased dramatically in the presence of alumina particles. When adsorbed onto micro-alumina, 50% of asphaltenes oxidized before 250 °C. In the case of nano-alumina, the oxidation was less rapid and 50% of asphaltenes oxidized beyond 250 °C (before 380 °C). Although the values of activation energies obtained for micro-alumina are comparable to that obtained for nano-alumina, a low-temperature regime shows a higher catalytic effect of micro-alumina toward asphaltene oxidation.

4. CONCLUSION

The adsorption and oxidation of asphaltenes onto two aluminas with different particle sizes and similar surface acidity were investigated to examine the effect of the particle size on asphaltene adsorption and catalytic oxidation. The adsorption isotherms were determined, and isotherm modeling was conducted using both the Langmuir and Freundlich isotherm models. Asphaltene adsorption onto nano-alumina was appropriately described by the Langmuir model, while micro-alumina better fit to the Freundlich model. On a surface area basis, the adsorption capacity of nano-alumina was higher than that of micro-alumina. This was attributed to the high extent of the dispersion degree of nanoparticles. On the other hand, micro-alumina showed higher catalytic activity toward asphaltene oxidation than nano-alumina. This enhanced catalytic effect demonstrated by micro-alumina shows that textural properties play an important role in catalysis.

AUTHOR INFORMATION

Corresponding Author

*Telephone: +1-403-210-9772. Fax: +1-403-210-3973. E-mail: nassar@ucalgary.ca.

ACKNOWLEDGMENT

Financial support provided by Carbon Management Canada, Inc. (CMC-NCE), a research network financed by the National Science and Engineering Research Council of Canada (NSERC), is gratefully acknowledged. Thanks are due to Mr. William Reid (Sorbent Technologies) for providing the micro-alumina particles and to Mr. AbdelLatif Eldood for providing the nC-7 asphaltene sample.

REFERENCES

(1) Gill, S. S.; Tsolakis, A.; Dearn, K. D.; Rodríguez-Fernández, J. Combustion characteristics and emissions of Fischer−Tropsch diesel fuels in IC engines. *Prog. Energy Combust. Sci.* **2011**, *37* (4), 503–523.

(2) Governement of Alberta. *Alberta Environmental Management of Alberta's Oil Sands*, 2009; http://environment.gov.ab.ca/info/library/8042.pdf.

(3) Nassar, N. N.; Hassan, A.; Pereira-Almao, P. Application of nanotechnology for heavy oil upgrading: Catalytic steam gasification/cracking of asphaltenes. *Energy Fuels* **2011**, *25* (4), 1566–1570.

(4) Nassar, N. N.; Hassan, A.; Pereira-Almao, P. Comparative oxidation of adsorbed asphaltenes onto transition metal oxide nanoparticles. *Colloids Surf., A* **2011**, *384*, 145–149.

(5) Nassar, N. N.; Hassan, A.; Pereira-Almao, P. Metal oxide nanoparticles for asphaltene adsorption and oxidation. *Energy Fuels* **2011**, *25* (3), 1017–1023.

(6) Chan-Remillard, S.; Kerr, D.; Marques, L. Applications of nanotechnology within the oil and gas industry. *Explor. Prod., Oil Gas Rev.* **2010**, *8* (2), 6–9.

(7) Nassar, N. N.; Pereira-Almao, P. Capturing $H_2S_{(g)}$ by in situ-prepared ultradispersed metal oxide particles in an oilsand-packed bed column. *Energy Fuels* **2010**, *24* (11), 5903–5906.

(8) Nassar, N. N.; Husein, M. M.; Pereira-Almao, P. Ultradispersed particles in heavy oil: Part II, sorption of $H_2S_{(g)}$. *Fuel Process. Technol.* **2010**, *91* (2), 169–174.

(9) Nassar, N. N.; Hassan, A.; Pereira-Almao, P. Effect of surface acidity and basicity of aluminas on asphaltene adsorption and oxidation. *J. Colloid Interface Sci.* **2011**, *360*, 233–238.

(10) Nassar, N. N. Asphaltene adsorption onto alumina nanoparticles: Kinetics and thermodynamic studies. *Energy Fuels* **2010**, *24* (8), 4116–4122.

(11) Montgomery, D. C.; Runger, G. C. *Applied Statistics and Probability for Engineers*, 4th ed.; John Wiley and Sons: New York, 2006.

(12) Webb, P. A.; Orr, C. *Analytical Methods in Fine Particle Technology*; Micrometrics Instruments: Norcross, GA, 1997.

(13) Coats, A. W.; Redfern, J. P. Kinetic parameters from thermogravimetric data. *Nature* **1964**, *201* (4914), 68–69.